CHEMICO-PHYSICAL PROPERTIES OF NANO-SIZED CERAMIC INKS FOR INK-JET PRINTING

D. Gardini(1), F. Matteucci(1), M. Blosi(1), A.L. Costa(1),
M. Dondi(1), C. Galassi(1), M. Raimondo(1)
G. Baldi(2), E. Cinotti(2)

(1)Institute of Science and Technology for Ceramics, Faenza, Italy
(2)Advanced Research Laboratory, Colorobbia Italia, Italy

ABSTRACT

This work is aimed at developing suitable nano-sized ceramic inks (nano-inks) for the ink-jet printing four-colour process. Nano-inks of different pigment composition were prepared with various solid loadings, and their chemico-physical properties, relevant for the ink-jet application, were measured. Moreover, penetration kinetics of the inks through different unfired ceramic tile bodies was experimentally appraised. Results show that pigment particle sizes are in the 10-90 nm range, and that all the nano-inks are stable for long time (i.e. more than one year) due to both their high values of ζ-potential and the steric effect of the dispersing medium. This high stability avoids problems of nozzle clogging which might arise from particle sedimentation. Most of nano-inks have a Newtonian behaviour with relatively low viscosities (<50 mPa s) even if, according to pigment composition, more concentrated nano-inks may have an excessive viscosity for ink-jet applications. Surface tension requirements for ink-jet printing (i.e. 35÷45 mN/m) are fulfilled by the tested nano-inks, although the values vary significantly with pigment loading. The electrical conductivity is, generally, in the 1-100 µS/cm range and is influenced by pigment composition (e.g. inks containing metallic particles exceed 1 S/cm). The penetration kinetics is mostly affected by pigment loading and composition, while it does not significantly depend on microstructure and composition of the two ceramic substrates considered. In conclusion, most of nano-inks investigated show satisfactory chemico-physical properties for ink-jet applications, as proved by preliminary tests. Those which are out of typical ranges can be enhanced by modifying the composition and/or the operating parameters.

1. INTRODUCTION

Decoration is aimed at increasing the aesthetic value of surfaces, which is pivotal in the production of traditional ceramics[1]. Ink-jet printing is a non-impact matrix method based on projecting ink droplets onto a surface[2]. There are two main kinds of ink-jet printers: continuous and impulse or drop on demand (DOD). In continuous printers the ink stream, once ejected from the orifice, is broken in droplets that are then selectively electrically charged; therefore, passing through an electrical field, the charged droplets can be deflected in a gutter for recirculation, while the uncharged ones directly spread on the substrate to form an image[3]. As far as DOD printers are concerned, ink droplets are ejected only when required, by the application of an electrical signal on the ceramic piezoelectric that mechanically moves, squeezing out the drops[4,5].

Many characteristics of ink-jet printing technology make it interesting for decoration of ceramic articles. In particular, as far as high resolution images are concerned, the fact that ink-jet technology involves the smallest droplets volumes, compared to other decorating technologies, permits a better control of image quality. Besides, customized products can be obtained at admissible costs; in fact, the change of the printed image is obtained without any substitution of mechanical parts, as happens in all other decoration technologies, but only through the change of the software input. Nevertheless, though ink-jet printing has been applied to ceramic decoration for a few years, until now it has not become a common technology in the ceramic industry. This delay is due to the severe requirements concerning ceramic pigments and inks. In the former case, the colorants for ceramic materials must be highly refractory, capable to withstand the chemical corrosion of liquid phases formed during the firing of bodies or glazes, and with suitable optical characteristics[6]. Therefore, not all the inorganic structures are suitable for ceramic decoration[7]. As far as inks are concerned, it must be pointed out that the quality of ink-jet images depends on the properties of inks (*i.e.* viscosity, surface tension) and substrates (*i.e.* mineralogical composition and porosity) and on their interaction (*i.e.* wettability, spreading, penetration)[4]. In particular, the control and optimisation of ink physical properties, such as viscosity and surface tension, are the most critical aspects in ink-jet printing technology. In fact, ink viscosity must be low enough to allow a fast ink flow through the printhead nozzles, under the gradient pressure arising from ceramic piezoelectric movement, and to enhance an easier penetration in the capillary channels of porous substrate. As far as surface tension is concerned, its value must be higher than 35 mN/m in order to permit the droplet ejection out of the orifice avoiding dripping by gravity[5].

Nowadays, ink-jet printing on ceramics is carried out by using either soluble dyes or micronized pigments. The former offer a limited colour saturation and palette, while the latter can cause nozzles clogging and dispersion instability, if particle size is not carefully controlled. These problems can be overcome through nano-sized ceramic inks (*nano-inks*), made of dispersions of nanometric particles in a liquid organic vehicle, that are able to increase the image quality ensuring a high reliability to the printing systems[8]. As is well known from literature, nanoscale crystalline materials can be synthesized through different chemical methods[9],[10] and among these, the so-called polyol process gained good results[11],[12],[13]. The nano-inks studied in the present research were obtained through the polyol method, which consists in dispersing the metal precursors in an alcohol or solvent with high boiling point, mainly glycols, and heating the batch over 100°C. In order to fulfil the four-colour process requirements, pigments which develop the four basic colours (Cyan, Magenta, Yellow and Black: CMYK) were synthesized, characterized and further tested.

2. MATERIALS AND METHODS

2.1. MATERIALS

Nano-sized ceramic inks able to give the basic colours for the ink-jet printing four-colour process were prepared (Advanced Research Laboratory, Colorobbia Italia, Sovigliana Vinci, Italy). They are suspensions of ceramic oxides or metals synthesized in an organic medium (glycol) by the polyol process. In particular:

I) cyan colour was obtained starting from two different precursors ($CoAl_2O_4$ and Co_xO_y) and the corresponding nano-inks are hereafter named Cyan 1 and Cyan 2, respectively;

II) magenta colour was obtained by a gold precursor (Magenta);

III) yellow colour was obtained by a titania precursor (Yellow), and

IV) black colour was obtained starting from two different precursors ($CoFe_2O_4$ and $FeCr_2O_4$) and the corresponding nano-inks are named Black 1 and Black 2, respectively.

The density of solid pigment (ρ_p) and the solid content, expressed in weight (ω_p) and in volume (ϕ_p), for these six nano-inks are reported in Tab. 1. In order to study the effect of pigment concentration, the Yellow ink was prepared at four different solid loadings ranging nominally from 1 to 12 wt%, while the Black 1 ink was prepared at five different solid contents up to nominal 28 wt%. Further, the Black 2 ink at 3 wt% was tested to investigate the influence of ζ-potential on penetration. These inks will hereafter be labelled with a suffix indicating the solid content following their names. The density values for the whole set of inks are reported in Tab. 2, which summarizes the samples analyzed.

NANO-INK	PIGMENT	ρ_p (g/cm³)	ω_p (%)	ϕ_p (%)
Cyan 1	$CoAl_2O_4$	4.42	8.0	2.16
Cyan 2	Co_xO_y	6.25	4.0	0.74
Magenta	Au	19.32	1.1	0.064
Yellow	TiO_2, Sb, Cr	4.25	12.0	3.47
Black 1	$CoFe_2O_4$	5.27	12.9	3.05
Black 2	$FeCr_2O_4$	5.06	12.0	2.93

Table 1. Compositions and densities of pigments and pigments loadings for basic nano-inks.

	ω_p (%)				
NANO-INK	**1**	**3**	**9**	**12**	**28**
Cyan 1			**1.14**		
Cyan 2		**1.14**			
Magenta	**1.12**				
Yellow	1.12	1.13	1.21	**1.26**	
Black 1	1.12	1.14	1.20	**1.23**	1.41
Black 2		1.13		**1.24**	

Table 2. Nano-inks densities (g/cm³). Density of glycol is 1.12 g/cm³. Basic nano-inks are in bold. The weight fractions are nominal.

The effect of the physico-chemical nature of ceramic substrates on penetration kinetics was taken into account considering two different body compositions: a typical industrial porcelain stoneware (A) and the same added with a glass ceramics (B). In addition, four forming pressures, ranging from 100 to 500 kg_f/cm^2, were applied to the body in order to obtain unfired tile with different pore size distribution.

2.2. EXPERIMENTAL METHODS

Nano-inks and porous ceramic substrates were characterized in order to determine the main properties affecting the process of ink-jet printing. As discussed in the introduction, shear viscosity and surface tension are the physical properties which play an important role both on the ejection of droplets from the printing head and in the process of ink penetration through the capillary pores of ceramic substrates. Electrical conductivity of nano-inks, relevant in continuous direct ceramic ink-jet printing (DCIJP) technology, was also measured. Besides the determination of these properties, the size and the ζ-potential of the solid nano-particles in glycol were determined, too. As far as ceramic substrates are concerned, the pore size distribution measurements were performed. Finally, the penetration kinetics of nano-inks on different unfired ceramic tile bodies were determined in order to study the reciprocal interaction between the nanometric suspensions and the porous media.

2.2.1. Shear viscosity

The shear viscosity of nano-inks was measured by a stress-controlled rotational rheometer equipped with a plate-plate geometry (Bohlin C-VOR 120, Malvern-Bohlin Instruments, Cirencester, UK). The diameter of the plates was 60 mm and the gap imposed between the plates was 500 μm. Flow curves at 25°C were determined increasing the shear stress from 0.1 to 10 Pa in 21 logarithmic steps and measuring the corresponding shear rates.

2.2.2. Surface tension

The surface tension of nano-inks was determined with an optical device provided with a CCD video camera with a resolution of 752x582 pixels and a rate of image acquisition of 25 frames per second (OCA 15+, DataPhysics Instruments, Filderstadt, Germany). Pendant drop method was used and flat needles of 1.65 mm of outer diameter were employed. An image acquisition software allowed to determine the outline of the hanging nano-inks drops, which were fitted by the Laplace-Young method. The calculation of the surface tension requires the knowledge of the density of the material, which has been previously measured by the gravimetric method. The fitting was performed on well-developed droplets (of about 14 μL volume) hanging to the needle.

2.2.3. Electrical conductivity

The electrical conductivity of nano-inks was measured with the dip conductivity probe (with a constant cell of 74.8) associated to an electroacoustic spectroscope (AcoustoSizer II, Colloidal Dynamics, Warwick, USA), previous calibration with 0.01 and 0.1 M KCl solutions.

2.2.4. Particle size distribution

The particle size distribution of pigments in nano-inks was measured:

I) by dynamic light scattering (DLS, ZetaSizer-NanoSeries, Malvern Instruments, Malvern, UK) performed on as-prepared inks pouring out quartz cuvette;

II) by transmission electron microscopy (TEM, Zeiss 109, Oberkochen, Germany) performed at 80 kV on dried powders placed on metallic grid.

2.2.5. ζ - potential

The ζ-potentials of pigments were measured by an electroacoustic method based on the measure of the Electrokinetic Sonic Amplitude (ESA) signal generated in the organic suspensions when an alternating electric field is applied (AcoustoSizer II, Colloidal Dynamics, Warwick, USA)[14]. The instrument determines the ζ-potential of the particles by fitting the volume average dynamic mobility over a range of 13 different frequencies (ranging from 1 to 18 MHz) of the alternate electric field imposed. The particle-size distribution, necessary for the fitting, is also measured by a sound attenuation technique. To obtain the particle contribution to the total attenuation the attenuation was measured in the glycol solvent and the result subtracted to the sample measurement (*background correction*). Data concern both the attenuation zeta potential (ζ potential) that is fitted with an attenuation-based particle size measurement, and the electrophoretic zeta potential (Hückel ζ potential) that is fitted with an ESA-based particle size measurement, calculated at a fixed frequency (1.3 MHz). Moreover, electrical conductivity (K) and mean particle size (d_{50}) obtained from electroacoustic measurements were reported, too.

2.2.6. Pore size distribution

The pore-size distribution of ceramic substrates was performed by mercury intrusion porosimetry on tile fragments with an apparent area around 2 cm^2 (ThermoFinnigan Pascal 140 and 240), assuming a mercury-samples contact angle of 140°.

2.2.7. Penetration tests

The penetration kinetics were determined with the same optical instrument used for the evaluation of surface tension, but using the sessile drop method. Droplets of 4 μL volume were dispensed from needles of 0.81 mm outer diameter and the substrate was moved toward the hanging droplet until they came in contact. The droplets were taken down from the surface forces and their shape evolution on substrates, due to penetration, was recorded starting from that instant. Fitting the outline of the droplets time by time (i.e., every 40 ms) with the Laplace-Young method, the mass fraction absorbed (M_a) with respect to the mass of the deposited nano-inks droplets (M_d) was measured, achieving a non dimensional penetration index (I_p), where $I_p = M_a / M_d$.

3. RESULTS AND DISCUSSION

3.1. SHEAR VISCOSITY

In the range of shear stresses investigated the nano-inks considered show a Newtonian behaviour with viscosities at 25°C ranging from about 40 to 200 mPa s, except the Cyan 1 ink which shows a viscosity decrease (shear-thinning behaviour) between 1 and 4 Pa s (Figure 1). These values are relatively high with respect to typical viscosities of inks employed in ink-jet printing[5]. Glycol, the dispersing medium, has a viscosity of about 24 mPa s at 25°C and is not possible to lower under this limit without changing the operating condition (*i.e.* temperature, dispersing medium). Cyan 2, Magenta and Black 1 inks have similar low viscosities (around 40 mPa s), although the Black 1 ink is fifty times more concentrated (as volume solid content) than Magenta. Yellow and Black 2 inks have a viscosity quite high (around 190 and 120 mPa s, respectively) and out of range of ink-jet applicability. In order to fulfil the ink-jet viscosity requirement one may exploit the possibility of ink-jet printing devices to operate at increasing temperature, therefore decreasing the ink viscosity. The shear-thinning behaviour of the Cyan 1 ink can be explained claiming some agglomeration phenomena among solid particles.

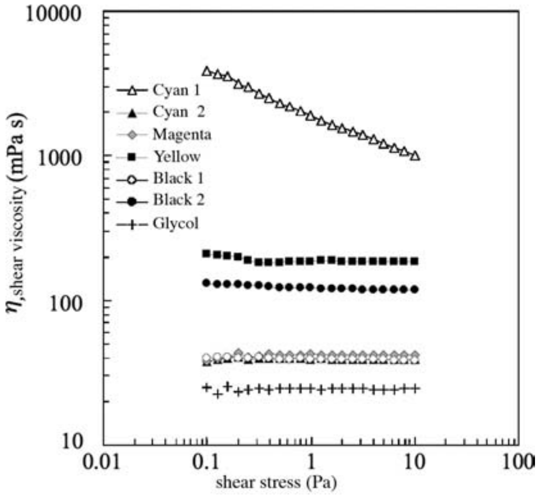

Figure 1. Flow curves for basic nano-inks. Viscosity of glycol is 24.4 mPa s.

The influence of solid content on shear viscosity of the Yellow and Black 1 inks is shown in Fig. 2. The Yellow ink increases its viscosity quickly from 24 to 185 mPa s passing from 1 to 12 wt% of solid load. Instead, the viscosity increase of Black 1 is very slow up to 28 wt%; at 12 wt% its viscosity is still lower than 40 mPa s. This suggests that the colloidal stability of the Yellow ink is worse than that of the Black 1 ink, *i.e.* the agglomeration phenomena are more favoured for titania particles with respect to $CoFe_2O_4$, as expected by practice with TiO_2 pigments[7].

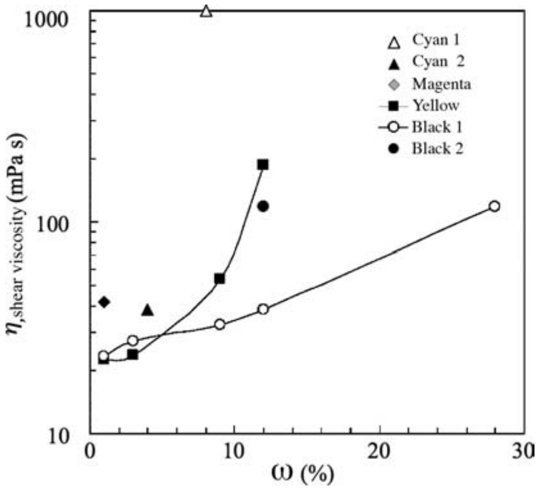

Figure 2. Effect of solid content on viscosity of Yellow and Black 1 inks.
Shear viscosities of Cyan 1 (at 10 s^{-1}), Cyan 2, Magenta and Black 2 inks are also reported.

3.2. SURFACE TENSION

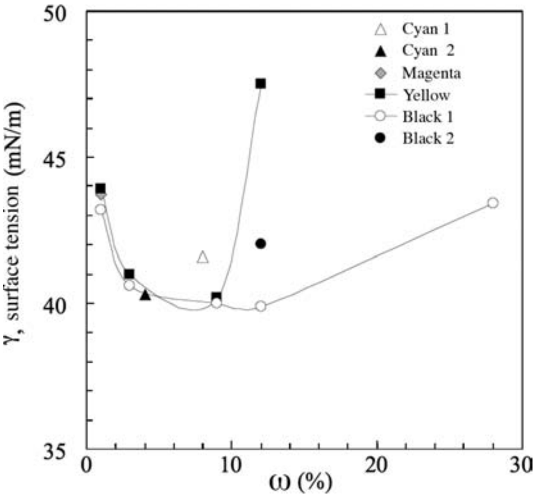

Figure 3. Effect of solid content on surface tension of Yellow and Black 1 inks. Surface tensions of Cyan 1, Cyan 2, Magenta and Black 2 inks are also reported

Surface tension values are shown in Figure 3. The equilibrium surface tension of a colloidal dispersion is not achieved instantaneously because the nano-particles diffuse to the interface and because of the continual contamination by the environment, therefore the surface tension values vary with droplet ageing[15]. In this research, in order to take the most reliable surface tension data for ink-jet printing, where drop formation and emission from printhead is very fast, the recorded values are referred to the first instant after the drop formation out of the needle. All the tested samples fulfil ink-jet requirements, except the Yellow ink at 12 wt%. The surface tension variation with particle loading is evident both in Yellow and Black 1 and its trend shows a decrease to a certain concentration followed by a fast increase at a peculiar higher concentration. This phenomenon is due to the spontaneous movement of the nanoparticles toward the ink-air interface, which causes a decrease of glycol molecules cohesion, therefore causing a decrease of the surface tension values. As shown in figure 3, this trend changes at a peculiar particle loading for each ink; in fact at this value the particle loading is so high that the capillary forces between the particles at the interface will prevail, therefore increasing the ink surface tension[15].

3.3. ELECTRICAL CONDUCTIVITY

As shown in Figure 4, the electrical conductivity values are in the range 1÷100 μS/cm for most of the inks, but the Magenta one. Therefore, only the latter is suitable for continuous ink-jet printing which requires values higher than 1000 μS/cm[16]. The particle loading affects the electrical conductivity of the Yellow inks, while the Black 1 exhibits values that remain almost constant. The high value of the Magenta ink is typical of a metal when the particle size is over 10 nm[17], as it is in our case (Table 3).

NANO-INK	η (mPa s)	γ (mN/m)	K (μS/cm)	d_{av} (nm)
Cyan 1	998	41.6	12.5	-
Cyan 2	38.8	40.3	10.0	-
Magenta	42.0	43.7	1420	92
Yellow (12 wt%)	185	47.5	88.0	19
Black 1 (12 wt%)	38.6	39.9	8.1	22
Black 2 (12 wt%)	118	42.0	6.8	47

Table 3. Viscosity (η), surface tension (γ), conductivity (K), and average size (d_{av}) from DLS for basic nano-inks.

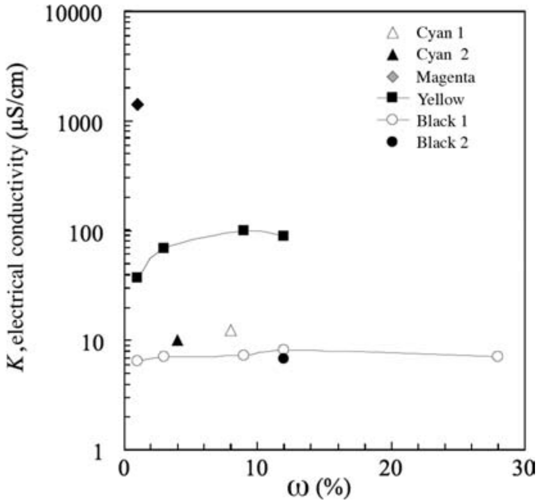

Figure 4. Effect of solids contents on electrical conductivity of Yellow and Black 1 inks. Electrical conductivities of Cyan 1, Cyan 2, Magenta and Black 2 inks are also reported

3.4. PARTICLE SIZE DISTRIBUTION

DLS measurements allowed to state that pigment sizes are comprised in the 10-90 nm range, therefore confirming the efficiency of the polyol method in synthesizing nanoparticles regardless pigment composition (Table 3). Due to the fact that wavelengths absorbance of DLS instrument is in the blue region, Cyan inks were analysed only by TEM. Particles size of Magenta ink are approximately in the 60-100 nm range as showed in Figure 5*a*, which is in accordance with DLS curve (Figure 5*b*). The higher the pigment amount the coarser the particle size; in fact, increasing pigment amount from 1 to 12 wt%, particle size grows from 5 to 19 nm for the Yellow ink and from 8 to 22 nm for the Black 1 ink. This phenomenon is probably due to particle agglomeration.

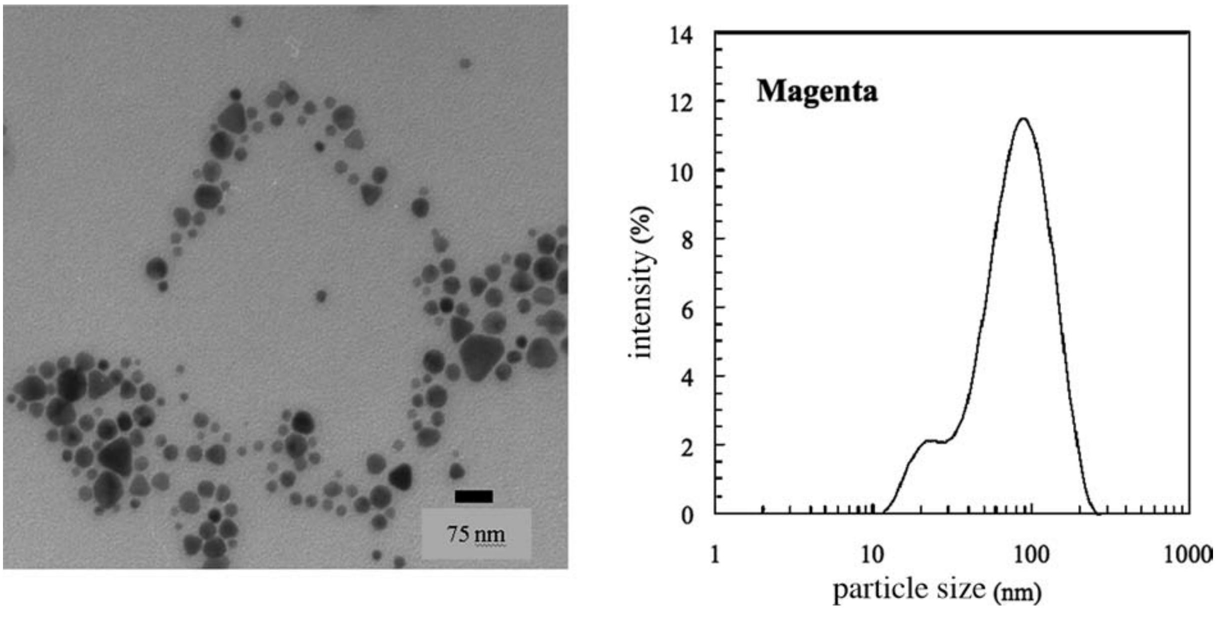

Figure 5. (a) TEM image and (b) particle-size distribution (DLS) for Magenta ink.

3.5. ζ-POTENTIAL

NANO-INK	ζ (mV)	ζ Hückel (mV)	K (μS/cm)	I_p
Black 1 (3 wt%)	29.7	28.4	10	0.2
Black 1 (12 wt%)	47.5	39.4	7	0.3
Black 2 (3 wt%)	18.9	19.5	55	0.7

Table 4. Electroacoustic characterization of Black nano-inks.

Data obtained by electroacoustic measurements on Black nano-inks are reported in Tab. 4. Provided that the attenuation size is not too large (d_{50} around 100 nm) comparable with diameter measured by the DLS technique, the attenuation zeta (ζ) can be considered steadier and more reliable than Hückel zeta (ζ Hückel). The positive sign of zeta potential indicates a proton transfer between the glycol and the basic surface sites of pigment oxides. The absolute values of ζ-potential depend also on the presence of other species that may come from the synthesis (*e.g.* water, surfactants) and so it justifies the fluctuation in the ζ potential absolute value of samples from the same batch but at different concentration. The first consideration that can be extrapolated from the data analysis is that the attenuation results are actually reliable only at higher concentration (≥ 10 wt%), but it is evident that the ζ-potential of Black 1 (12 wt%) is higher than that of the Black 1 (3 wt%). This behaviour can be related to the slightly higher value of the penetration index ($I_p = 0.3$) of Black 1 (12 wt%) in comparison with Black 1 (3 wt.%) ($I_p = 0.2$) that can be attributed to the better electrostatic stabilization of the former. From the analysis of the dynamic mobility spectrum, Black 2 (3 wt%) sample shows a smaller mobility at low frequency compared to that of both Black 1 samples. Besides, the mobility magnitude of Black 2 (3 wt%) increases with frequency where both Black 1 mobilities are flat. This result suggests that sample Black 2 (3 wt%) may contain polymers adsorbed on the surface giving a steric stabilization, which is coherent with the highest penetration index measured ($I_p = 0.7$). The electrical conductivity value confirms the presence of some additive in the Black 2 (3 wt%) ink that presents the highest conductivity. From this preliminary electroacoustic characterization of nanometric inks dispersed in glycol it can be concluded that an electrostatic or steric stabilization of particles can improve the penetration index. A further investigation is needed to confirm this correlation. For this reason the electroacoustic characterization could be a suitable tool to predict the technological behaviour of inks.

3.6. PORE-SIZE DISTRIBUTION OF SUBSTRATES

The pore-size distributions of the A and B substrates are shown in Figure 6. Obviously, increasing the forming pressure both the open porosity and the pore diameter decrease, but the trend is slightly different depending on body composition. In fact, the glass-ceramic addition (body B) determined a peculiar tendency with the forming pressure as highlighted by the abrupt decrease of pore diameter stepping from B 100 to B 300 and by overlapping of B 300 with B 500 at the lowest values of pore size. The range of variation in pore diameters is very limited, being in between 0.25 and 0.43 μm. Besides, bodies B showed higher values than the A ones, but for the highest forming pressure (Table 5).

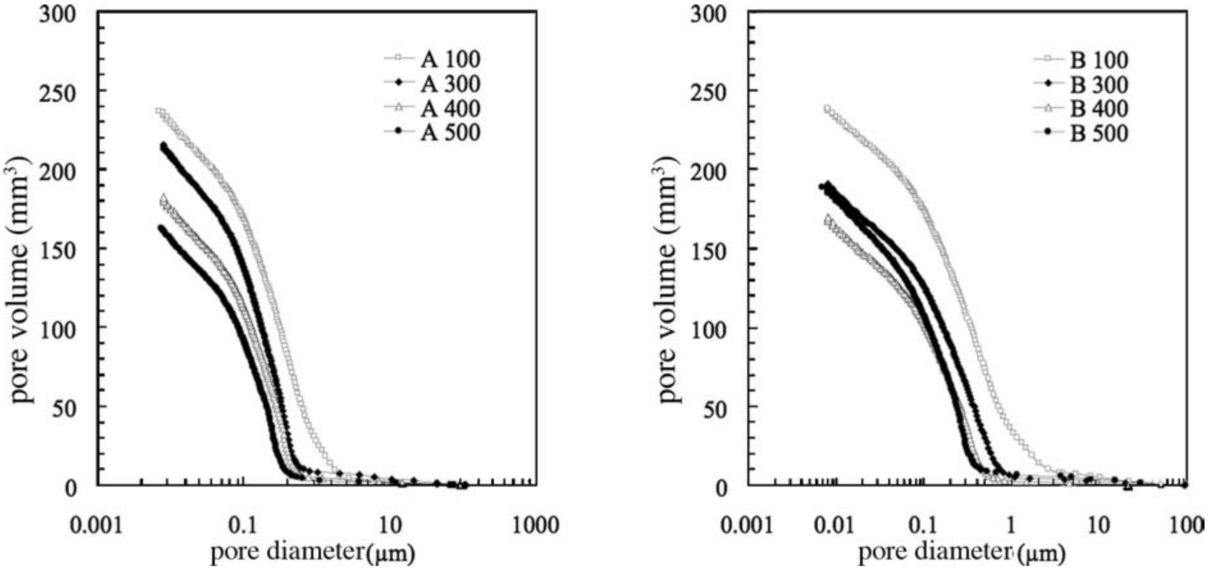

Figure 6. Pore-size distribution of ceramic substrates.

	FORMING PRESSURE (kgf/cm²)			
SUBSTRATE	100	300	400	500
A	0.39	0.37	0.28	0.26
B	0.43	0.36	0.31	0.25

Table 5. Average pore diameters (mode) of porous substrates (µm).

3.7. PENETRATION TESTS

The penetration behaviour of nano-inks on ceramic substrates depends on the physical properties of the inks and on the tile characteristics. In this work the penetrability of the nano-inks was tested on substrates with different phase composition and pore size distribution. In particular, two different substrates – a typical porcelain stoneware (A) and the same added with a glass-ceramics (B) – formed at four different pressures, ranging from 100 to 500 kg_f /cm^2, were considered. While the kind of substrate does not significantly affect the penetration kinetics, the forming pressure does influence the degree of penetration. In fact, at increasing forming pressure, the pore-size distribution shifts towards lower values (Figure 6). Consequently the penetration through the porous media becomes more difficult because a higher pressure gradient is needed to overcome the surface tension. As the penetration is not affected by the chemical composition of substrates and the worst penetration occurs with the smallest pore size, in order to evaluate the effect of particle content only the ceramic substrate B 500 was chosen.

An increased particle loading enhances the probability of agglomeration phenomena, therefore determining not only an increase of ink viscosity and particle size, but also a decrease of the ink penetration index, previously defined. As it is appreciable in Figure 7*a*, the Yellow ink presents a slower penetration rate at increasing concentration. The penetration index after 3 s is lower than 0.3 for all the Yellow inks, that means that only 30 % of the ink entered into the substrate. This low rate cannot be fully explained neither by clogging of pores nor by pore flooding. In fact, the particle size is one order of magnitude smaller than the average pore diameter and the pure glycol penetration index is approximately 0.8 (Figure 7*b*); therefore the pigment loading causes the low penetration of the ink. It can be stated that nanoparticles affect ink properties, such as viscosity and surface tension, as well as the interaction between ink and substrate, so reducing the penetration.

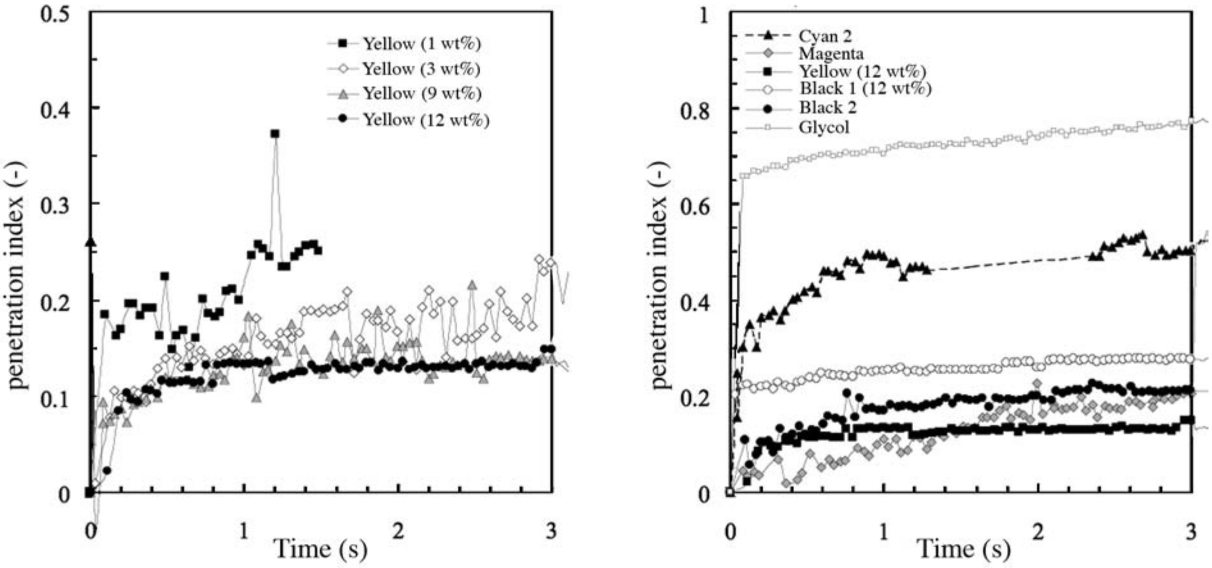

Figure 7. Kinetics of penetration of Yellow inks (a) and of the basic nanoinks (b) on B 500 substrate.

Finally, with the purpose to differentiate the affinities of the basic nano-inks with respect to the substrate, a comparison of penetration kinetics is shown in Figure 7*b*. As aforementioned, glycol exhibits the quickest penetration, while the Yellow ink has the lowest index; Cyan 2 is peculiar, being its penetration index twice all the other inks tested.

4. CONCLUSIONS

Highly stable ceramic inks were prepared by the polyol method, allowing obtaining pigments with actually nanometric size (*i.e.* 10-90 nm) based on metallic gold or spinel-like or rutile-like stoichiometries. These pigments develop vivid colours approaching the yellow, cyan, magenta and black required for the four-colour printing process. A wide-ranging characterization, including shear viscosity, surface tension, electrical conductivity, ζ–potentials, proved these inks do fulfil the requirements for drop-on-demand ink-jet printing. Some non-optimal behaviours can be corrected by using appropriate additives and/or increasing the ink temperature prior to the ejection. The physico-chemical properties of inks depend on the concentration and chemical nature of pigments as well as on the occurrence of synthesis by-products (*e.g.* water). Penetration of inks into the green ceramic substrate is affected by both the volume and size of pores, being promoted by lower forming pressures. In some cases, the penetration rate suffered by agglomeration phenomena, which are appreciable when pigment load is high, particularly for titania-based dyes. Preliminary testing demonstrates that these nanosized ceramic inks are fully suitable for the four-colour ink-jet printing. Further work will optimise the ink-jet application and will investigate which phenomena occur and mostly influence the penetration kinetics.

REFERENCES

[1] AA.VV., *Glazing and Decoration of Ceramic Tiles*, Sala Publisher, Modena, (2000).

[2] H.R. Kang, "Water-Based Ink-Jet Ink. I. Formulation," *J. Imag. Sci.*, **35** (1991) 179-188.

[3] A. Atkinson, J. Doorbar, A. Hudd, D.L. Segal, P.J. White, "Continuous Ink-Jet Printing Using Sol-Gel "Ceramic" Inks," *J. Sol-gel Tech.*, **8** (1997) 1093-1097.

[4] H.P. Le, "Progress and Trends in Ink-jet Printing Technology," *J. Imaging Sci. Technol.*, **42** (1998) 49-62.

[5] P. Calvert, "Inkjet Printing for Materials and Devices," *Chem. Mater.*, **13** (2001) 3299-3305.

[6] A.L. Costa, G. Cruciani, M. Dondi, F. Matteucci, "New outlook on ceramic pigments," *Ind. Cer.*, **23** (2003) 1-11.

[7] R. A. Eppler, "Selecting Ceramic Pigments," *Am. Ceram. Bull.*, **66** (11) (1987) 1600-1604.

[8] G. Baldi, M. Bitossi, A. Barzanti, Patent WO 03/076521 A1 (2003).

[9] M. Fenandez-Garcia, A. Martinez-Arias, J.C. Hanson, J.A. Rodriguez, "Nanostructured Oxides in Chemistry Characterization and Properties," *Chem. Rev.*, **104** (2004) 4063-4104.

[10] C.N.R. Rao, A. Müller, A.K. Cheetham, *The Chemistry of Nanomaterials. Synthesis, Properties and Applications*, Wiley-VCH, vols. **1-3** (2005).

[11] C. Feldmann, H.-O. Jungk, "Polyol-Mediated Preparation of Nanoscale Oxide Particles," *Angew. Chem. Int. Ed.*, **40** (2001) 359-362.

[12] C. Feldamann, J. Merikhi, H.-O. Jungk, "Sub-Micrometer $CoAl_2O_4$ Pigment Particles Synthesis and Preparation of Coating," *J. Mater. Chem.*, **10** (2000) 1311-1314.

[13] L. Poul, S. Ammar, N. Jouini, F. Fiévet, F. Villain, "Synthesis of Inorganic Compounds (Metal, Oxide and Hydroxide) in Polyol Medium: A Versatile Route Related to the Sol-Gel Process," *J. Sol-Gel Sci. Tech.*, **26** (2003) 261-265.

[14] R.J. Hunter, "Review: Recent Developments in the Electroacoustic Characterisation of Colloidal Suspensions and Emulsions," *Colloids and Surfaces A*, **141** (1998) 37-65.

[15] L. Dong, D. Johnson, "Surface Tension of Charge-Stabilized Colloidal Suspensions at the Water-Air Interface," *Langmuir*, **19** (2003) 10205-10209.

[16] W.D. Teng, M.J. Edirisinghe, "Development of Ceramic Inks for Ink Jet Printing: Effect of Conductivity," *Key Engineering Materials*, **132-136** (1997) 337-340.

[17] C.N.R. Rao, G.U. Kulkarni, P.J. Thomas, P.P. Edwards, *Chem. Eur. J.*, **8** (2002) 28-35.